Article

Marginal and Internal Fit of Monolithic Zirconia Crowns Fabricated by Using Two Different CAD-CAM Workflows: An In Vitro Study

Vahap Çin [1], Ayça Deniz İzgi [1], Ediz Kale [2] and Burak Yilmaz [3,4,5,*]

1   Department of Prosthodontics, Faculty of Dentistry, Dicle University, Diyarbakir 21200, Turkey
2   Department of Prosthodontics, Faculty of Dentistry, Mersin University, Mersin 33343, Turkey
3   Department of Reconstructive Dentistry and Gerodontology, School of Dental Medicine, University of Bern, Freiburgstrasse 7, 3010 Bern, Switzerland
4   Department of Restorative, Preventive and Paediatric Dentistry, School of Dental Medicine, University of Bern, Freiburgstrasse 7, 3010 Bern, Switzerland
5   Division of Restorative and Prosthetic Dentistry, The Ohio State University, Columbus, OH 43210, USA
*   Correspondence: burak.yilmaz@zmk.unibe.ch

Abstract: Objectives: Few studies have evaluated the marginal fit of computer-aided design—computer-aided manufacturing (CAD-CAM) monolithic zirconia crowns fabricated through completely digital workflow; however, the internal fit of these restorations is not well known. The purpose of this in vitro study was to evaluate the marginal and internal fit of monolithic zirconia crowns fabricated by using digital workflow, including intraoral scanner (IOS) scans, and compare the results to those of a semi-digital workflow, which combined conventional impressions, poured casts, and extraoral scanner (EOS) scanning. Materials and methods: A typodont right mandibular first molar was prepared for a complete-coverage ceramic crown and scanned using an IOS. The conventional impressions of the preparation were also made, and stone casts were poured and scanned by using an EOS. Virtual models were generated for both workflows, and identical virtual anatomic contour crowns were designed using CAD software. Monolithic zirconia crowns were fabricated for both IOS (ZI; $n = 10$) and EOS (ZE; $n = 10$) groups. The silicon replica technique was used to evaluate the marginal and internal fit of the crowns. Measurements were made at 13 points on buccolingual and mesiodistal cross-sections per specimen with a $\times 6.5$ to $\times 50$ zoom stereo microscope. The results from both groups were statistically compared using the Independent Samples *t*-tests and the Mann–Whitney U test ($\alpha = 0.05$). Results: Mean gap values at all measurement locations for ZE were significantly higher than those for ZI ($p \leq 0.002$). Overall mean values ranged between 29 and 43 μm (median: 28–42 μm) for ZI and 42 and 75 μm (median: 43–77 μm) for ZE. Conclusion: Completely digital workflow through intraoral scans provided significantly better marginal and internal fit for CAD-CAM monolithic zirconia crowns compared with the semi-digital workflow, where stone casts obtained from conventional impressions were scanned with an EOS. Yet, both workflows provided an acceptable marginal and internal fit for CAD-CAM monolithic zirconia molar crowns (<120 μm). Clinical Relevance: Completely digital workflow using IOS scans may be advantageous for the fabrication of CAD-CAM monolithic zirconia crowns as favorable results can be obtained with less material waste and potentially shortened overall treatment time as the impression files can be transferred to the production facility electronically. The results need to be corroborated with clinical studies.

Keywords: marginal fit; internal fit; zirconia; CAD-CAM; IOS; replica technique

1. Introduction

Three-dimensional (3D) intraoral scanners (IOSs) have enabled the fabrication of completely digital indirect restorations using computer-aided design—computer-aided

manufacturing (CAD-CAM) technology [1,2]. Although still not affordable by every practice and having insufficiencies related to accuracy for long-span fixed dental prostheses (FDPs) [2], IOSs have advantages over semi-digital workflow, which incorporates extraoral scanners (EOSs) to scan stone casts obtained from conventional impressions. IOSs eliminate impression and solid cast materials, improve patient comfort, enable rapid data transfer to the laboratory for fabrication, and shortened overall treatment time [3,4], especially when monolithic crowns are fabricated in the posterior [5], where aesthetics is not a priority [6]. In this respect, IOSs are replacing conventional impressions preceded by CAD-CAM workflow that includes 3D extraoral (laboratory) scanners.

With their improved physical properties [7–11], biocompatibility [8,10,12], reduced plaque accumulation [12], and aesthetic appearance, CAD-CAM monolithic zirconia crowns have the potential to outperform and permanently replace metal–ceramic posterior crowns [13]. Nevertheless, results on the clinical performance of monolithic zirconia crowns are currently limited to short-term follow-ups [6,14,15].

The fit of a crown is crucial for its clinical success [16]. Marginal misfit may lead to excessive plaque accumulation, microleakage, and cement breakdown, therefore increasing the risk of secondary caries, periodontal disease, pulpal inflammation, and impaired retention of the restoration [17–21]. Internal fit is directly associated with the retention and resistance properties of crowns [22]. Larger misfit values decrease retention and increase the risk of fracture under loads [23]. Uniformly distributed internal cement space is crucial for proper force dissipation under occlusal forces and protects the crown against loss of retention and potential fracture [24]. However, a clear scientific consensus on an acceptable range for internal and marginal discrepancy from a clinical perspective has not been reached yet.

The term internal gap corresponds to the shortest distance measured between the intaglio surface of a crown and the axial wall of the prepared abutment, and the same distance measured at the finish line of the preparation corresponds to the term marginal gap [25]. The shortest distance measured between the finish line of the preparation and the margin of the crown is called the absolute marginal gap and is defined as the vectorial combination of the marginal gap and the horizontal over- or under-extension of the restoration margin in relation to the preparation finish line [26]. At present, studies seem to be in agreement that any misfit at the margin of FDPs should be smaller than 120 μm [27–29]. Some suggest that this limit should not exceed 100 μm when CAD-CAM technology is involved [30,31]. As for the internal aspect of the restorations, it has been advocated that gaps between 100 and 300 μm could be considered clinically acceptable [32].

There are previous studies that evaluated the effect of a completely digital workflow on the fit of zirconia crown copings [33–36]. However, zirconia copings need to undergo a veneering process before cementation, which may compromise the fit of the final crown [37–39]. In addition, thickness has been shown as a factor that may affect the marginal fit of zirconia restorations, and the fit may differ between monolithic crowns and copings as their thickness differ [40]. Furthermore, monolithic zirconia crowns can be cemented after glazing or polishing without veneering, which may alter their final fit. In this regard, only two studies [41,42] have evaluated the marginal fit of monolithic zirconia crowns fabricated through a completely digital workflow by using IOSs. These studies only focused on the marginal fit of monolithic zirconia crowns, and to the authors' knowledge, there is a limited number of studies on the internal fit of monolithic zirconia crowns fabricated by using a completely digital workflow.

The purpose of this in vitro study was to evaluate the marginal and internal fit of CAD-CAM monolithic zirconia crowns fabricated by using a completely digital workflow and compare the results to those from a semi-digital workflow that combines conventional impressions, poured casts, and EOS scanning. The null hypothesis was that there would be no significant difference in the marginal and internal fit of crowns fabricated with two different workflows.

2. Materials and Methods

A right mandibular first molar typodont tooth (ANA-4 ZP; Frasaco, Tettnang, Germany) mounted on a typodont model (ANA-4 V CER; Frasaco, Tettnang, Germany) was prepared for a complete-coverage ceramic crown with 2 mm occlusal reduction, 1.5 mm axial reduction and 360-degree 1 mm deep chamfer margin [43]. The model was then scanned using a 3D IOS (CEREC AC Omnicam; Sirona Dental Systems, Bensheim, Germany) according to the manufacturer's recommendations (starting from the prepared tooth following on mandibular and maxillary arch, respectively, finalizing with a maxillomandibular registration) 10 times to generate 10 individual virtual 3D mandibular and maxillary casts in STL (stereolithography) format (Figure 1).

Figure 1. Occlusal virtual view of prepared typodont tooth on the mandibular model generated through digital impression making using IOS (CEREC AC Omnicam) (**a**); bite registration of virtual typodont full-mouth model (**b**); occlusal virtual view of preparation site on CAD image software (CEREC Software) (**c**); occlusal virtual view of designed crown restoration (**d**). IOS intraoral scanner; CAD computer-aided design.

Conventional impressions of the model were also made using vinyl-polysiloxane impression material (Elite HD+; Zhermack, Rovigo, Italy) with a one-step dual-phase technique (putty-soft and light-body) 10 times, and 10 pairs of stone casts (mandibular and maxillary) were poured in dental stone. Then, the casts were scanned with a 3D EOS (inEos X5; Sirona Dental Systems, Bensheim, Germany) according to the manufacturer's recommendations to generate 10 virtual 3D mandibular and maxillary casts along with their respective maxillomandibular registration (Figure 2). A virtual anatomic-contour crown with a simulated cement space of 40 μm was designed and converted to STL format for each virtually generated model of the molar tooth using IOS (CEREC SW 5.0; Sirona Dental Systems, Bensheim, Germany) and EOS (inLab CAD SW 20.0; Sirona Dental Systems, Bensheim, Germany) compatible CAD software programs. The designed crown data were used to mill 10 monolithic zirconia crowns for the IOS group (ZI; *n* = 10) and 10 monolithic zirconia crowns for the EOS group (ZE; *n* = 10) from pre-sintered zirconia blocks (inCoris TZI C-A2 16 mm; Sirona Dental Systems, Bensheim, Germany) with a CAM software (inLab CAD SW 20.0; Sirona Dental Systems, Bensheim, Germany) and a CAM dental milling-device (inLab MC X5; Sirona Dental Systems, Bensheim, Germany). The milled crowns were sintered (inFire HTC speed; Sirona Dental Systems, Bensheim, Germany) at 1500 °C for 20 min and glazed (Celtra Universal Overglaze; Sirona Dental Systems,

Bensheim, Germany) at 850 °C (Programat P510; Ivoclar Vivadent, Schaan, Liechtenstein) for 12 min according to the manufacturer's recommendations.
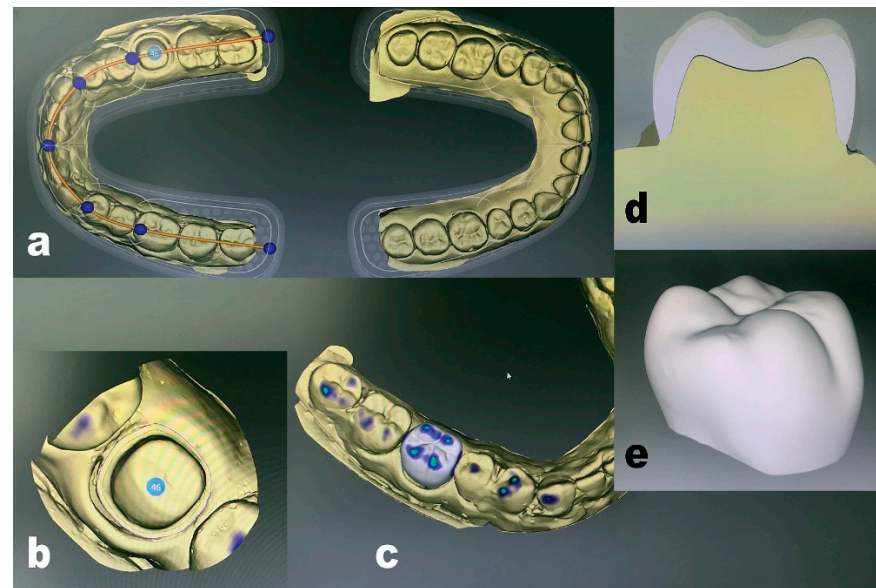

Figure 2. Occlusal virtual view on CAD image software (inLab CAD Software) of mandibular and maxillary typodont model generated through solid cast scanning using EOS (inEos X5) (**a**); occlusal virtual view of preparation site on CAD image software (**b**); occlusal virtual view of designed crown restoration (**c**); STL image of designed crown restoration during cement space setting on CAD image software (**d**); STL image of designed crown restoration (**e**). CAD computer-aided design; EOS extraoral scanner; STL standard tessellation language.

A two-dimensional (2D) silicon replica technique was used to evaluate the marginal and internal fit of all crowns [44]. The intaglio surface of the crowns was left unaltered after milling. Each crown was filled with light-body vinyl-polysiloxane impression material (Elite HD+; Zhermack, Rovigo, Italy) and seated on the prepared typodont tooth with maximum index finger pressure (180-degree distal pad press) applied for 5 s [45], and left in place under constant pressure of 10 N for 5 min, using static load equipment, until the silicon material set [32,46,47]. Crowns were removed carefully from the typodont model with the silicone replica obtained after filling the gap between the crown and the prepared tooth. Then, the crowns were filled with putty vinyl-polysiloxane impression material (Elite HD+; Zhermack, Rovigo, Italy) to support the shape of the replica specimens to be evaluated. After polymerization of the putty impression material, the specimens were removed from the crowns and carefully sectioned at the midline in buccolingual and mesiodistal directions (Figure 3) [44]. The thickness of the cross-section of the silicone replica standing for the cement material used in clinical practice [48] was measured at 13 measurement points on a buccolingual and mesiodistal section side. Five of the points were used for occlusal gap evaluation at 5 different locations (O1, O2, O3, O4, and O5), 3 pairs with corresponding points were used for axial (internal) gap evaluation at 3 other locations (AOA; axio-occlusal-angle, A; axial, AMA; axio-marginal-angle), and another pair with corresponding points were used for marginal gap evaluation at the marginal location (M) (Figures 4 and 5) [44,49]. All evaluations were done by a single operator by using a ×6.5 to ×50 zoom stereo microscope (Zeiss Stemi 2000-C; Carl Zeiss Microscopy GmbH, Jena, Germany) equipped with a 5-MP digital camera (AxioCam ERc 5s; Carl Zeiss Microscopy GmbH, Gottingen, Germany) and double-gooseneck light-emitting diode cold-light source (Zeiss KL200; Carl Zeiss Microscopy GmbH, Jena, Germany). A total of 520 measurements were made using digital imaging software (ZEN lite; Carl Zeiss Microscopy GmbH, Jena, Germany) in 2 groups (ZI and ZE) of 10 specimens. The means were calculated for every

measurement location, and the results were statistically compared between the groups. A uniformity index (UI) analyzing how uniform the internal fit of the crowns [50] obtained from occlusal and axial locations means ratio was also compared [49]. The Independent Samples *t*-tests and the Mann–Whitney U test was applied accordingly at a significance level of $\alpha = 0.05$ by using statistical software (IBM SPSS Statistics, v21.0; IBM Corp, Armonk, NY, USA) following the Shapiro–Wilk test of normality and Levene Statistic of homogeneity of variance. Post-statistical power analysis was also performed on the results revealing a power equal to 1 (0.926–1.000) with type I error at $\alpha = 0.05$.
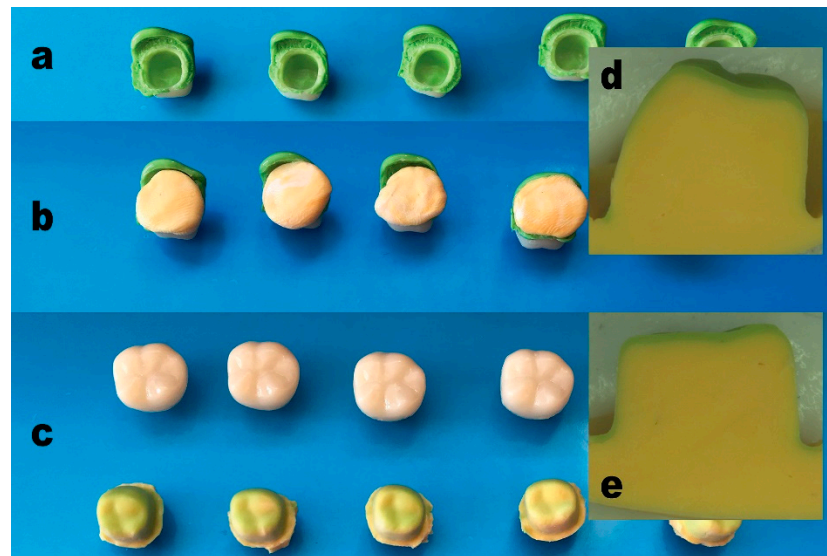
Figure 3. Intaglio surface view of crowns with silicone replica after filling the gap between restoration and prepared tooth (**a**); crowns filled with putty vinyl-polysiloxane impression material to support the shape of replica specimens (**b**); specimens removed from crowns after polymerization of putty impression material (**c**) specimen sectioned at the midline in buccolingual direction (**d**); specimen sectioned at the midline in mesiodistal direction (**e**).
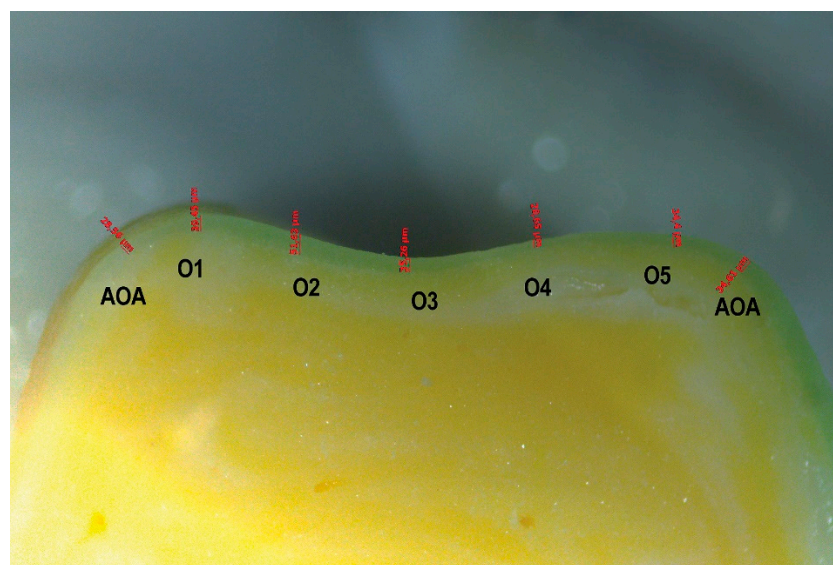
Figure 4. Occlusal gap evaluation location O1, O2, O3, O4, and O5, and one pair of measurement points for location AOA (mesiodistal direction micro view, original magnification ×50). O1 occlusal 1; O2 occlusal 2; O3 occlusal 3; O4 occlusal 4; O5 occlusal 5; AOA axio-occlusal-angle.
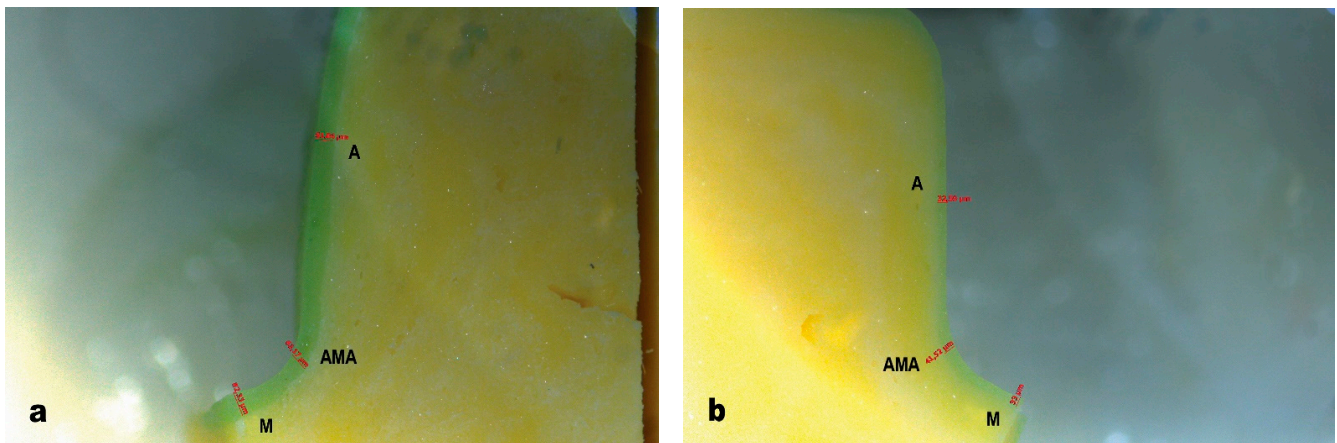
Figure 5. (**a**) Micro view of measurement points at locations A, AMA, and M (buccolingual direction, original magnification ×50). (**b**) Micro view of measurement points at locations A, AMA, and M (mesiodistal direction, original magnification ×50). A axial; AMA axio-marginal-angle; M marginal.

3. Results

The Independent Samples *t*-tests and the Mann–Whitney U test revealed that there was a statistical difference between the groups. The mean gap values at all measurement locations were significantly higher for group ZE than those for group ZI ($p \leq 0.002$) (Tables 1 and 2).

Table 1. Independent Samples *t*-test results for measurement location(s) with satisfied normality assumptions of individual measurement data ($p \leq 0.001$).

Location	*t*	*df*	*p*-Value	Mean Difference	Std. E.	95% CI Lower	95% CI Upper
M	3.793	18	0.001 *	12.4	3.269	5.531	19.269
AMA	6.548	18	0.000 *	18.9	2.886	12.836	24.964
AOA	4.844	10.738	0.001 *	19.8	4.088	10.776	28.824
O1	5.031	12.71	0.000 *	27.7	5.506	15.777	39.623
O2	7.044	11.874	0.000 *	30.8	4.373	21.262	40.338
O3	5.527	10.379	0.000 *	35.4	6.405	21.199	49.601
O4	4.360	18	0.000 *	30.1	6.903	15.598	44.602
O5	5.207	18	0.000 *	24.4	4.686	14.556	34.244

M marginal; AMA axio-marginal-angle; AOA axio-occlusal-angle; O1 occlusal 1; O2 occlusal 2; O3 occlusal 3; O4 occlusal 4; O5 occlusal 5; * indicates significance ($p < 0.05$).

Table 2. Mann–Whitney U test results for measurement location(s) with non-satisfied normality assumptions of individual measurement data ($p = 0.002$).

| Location	Group	Mean Rank	Sum of Ranks	*U*	*p*-Value
A	ZI	6.35	63.50	8.5	0.002 *
	ZE	14.65	146.50		

A axial; * indicates significance ($p < 0.05$).

The calculated mean gap values and standard deviations, median values, standard error, and minimum and maximum range values for both groups are presented in Table 3 (Figure 6). The calculated mean gap values, along with the minimum and maximum gap values individually measured at each measurement location for a specimen in a group, are also given in Tables 4 and 5.

Table 3. Mean gap values and standard deviations, median values, standard error, and minimum and maximum range values for group ZI and ZE (µm).

Location	Group	Mean	Std. D.	Median	Std. E.	Min.	Max.
M	ZI	29	6	32	2	19	37
	ZE	42	9	43	3	31	55
AMA	ZI	29	5	28	2	23	41
	ZE	48	7	45	2	37	58
A	ZI	36	5	36	2	26	44
	ZE	47	9	45	3	39	68
AOA	ZI	32	4	31	1	27	39
	ZE	52	12	49	4	38	74
O1	ZI	39	7	38	2	29	54
	ZE	66	16	64	5	46	92
O2	ZI	43	5	42	2	31	49
	ZE	73	13	77	4	55	92
O3	ZI	39	5	39	2	32	50
	ZE	75	20	72	6	47	112
O4	ZI	35	8	34	3	26	52
	ZE	65	20	60	6	42	107
O5	ZI	39	9	36	3	29	57
	ZE	64	12	65	4	47	84

M marginal; AMA axio-marginal-angle; A axial; AOA axio-occlusal-angle; O1 occlusal 1; O2 occlusal 2; O3 occlusal 3; O4 occlusal 4; O5 occlusal 5.
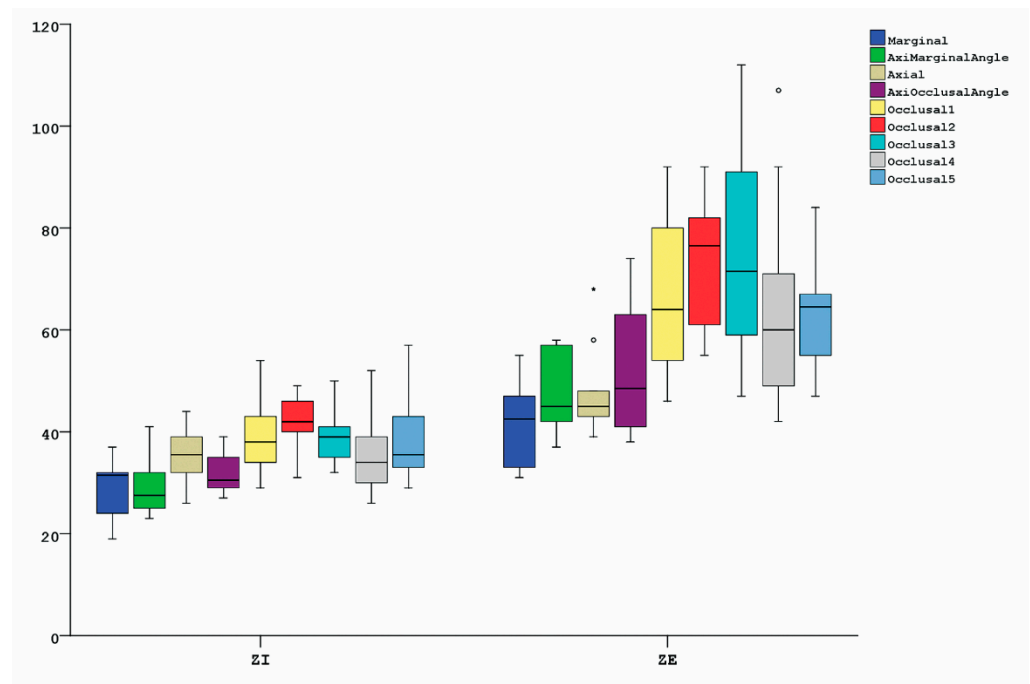
Figure 6. Gap evaluation results for compared groups (ZI and ZE) (µm).

Table 4. Mean gap values and minimum-maximum of individually measured gap values (in parentheses) for specimens in group ZI (*n* = 10) per measurement location (μm).

|	M	AMA	A	AOA	O1	O2	O3	O4	O5
#1	32 (20–41)	41 (24–62)	36 (15–59)	29 (23–41)	30 (28;31)	42 (37;46)	41 (40;42)	33 (33;34)	34 (30;38)
#2	30 (20–41)	30 (19–38)	35 (17–59)	27 (21–37)	36 (30;42)	46 (34;58)	38 (33;44)	36 (35;37)	39 (39;40)
#3	23 (14–35)	26 (12–40)	31 (15–45)	30 (18–41)	37 (30;45)	42 (33;52)	35 (30;40)	30 (28;33)	36 (30;42)
#4	19 (10–40)	25 (5–42)	26 (16–52)	31 (22–40)	42 (37;46)	46 (43;49)	50 (46;53)	45 (36;54)	53 (53;54)
#5	24 (12–54)	24 (18–28)	32 (17–46)	28 (18–36)	29 (27;31)	31 (25;37)	39 (35;42)	39 (28;49)	35 (30;40)
#6	32 (20–45)	32 (15–40)	39 (19–70)	36 (33–41)	43 (30;56)	48 (33;64)	39 (28;49)	35 (30;40)	43 (40;46)
#7	32 (16–70)	23 (17–33)	44 (21–78)	35 (28–44)	43 (42;45)	42 (38;47)	32 (26;38)	52 (40;64)	57 (37;76)
#8	37 (17–66)	32 (14–44)	39 (13–61)	39 (27–50)	54 (49;58)	49 (40;59)	46 (44;49)	26 (26;26)	33 (31;35)
#9	34 (15–65)	26 (15–35)	40 (26–62)	30 (29–35)	34 (28;40)	40 (27;52)	34 (33;35)	26 (21;31)	29 (23;34)
#10	31 (17–47)	29 (20–37)	33 (21–40)	33 (27–38)	39 (35;43)	40 (38;43)	39 (35;42)	31 (29;33)	33 (31;34)

M marginal; AMA axio-marginal-angle; A axial; AOA axio-occlusal-angle; O1 occlusal 1; O2 occlusal 2; O3 occlusal 3; O4 occlusal 4; O5 occlusal 5.

Table 5. Mean gap values and a minimum–maximum of individually measured gap values (in parentheses) for specimens in group ZE (*n* = 10) per measurement location (μm).

	M	AMA	A	AOA	O1	O2	O3	O4	O5
#1	53 (30–79)	57 (29–74)	48 (40–64)	63 (39–66)	81 (71;91)	82 (73;92)	70 (63;77)	58 (42;74)	53 (37;70)
#2	32 (14–46)	42 (23–61)	46 (33–64)	41 (27–57)	49 (43;56)	55 (44;67)	47 (37;58)	49 (44;53)	47 (45;49)
#3	31 (20–43)	42 (27–60)	44 (37–56)	43 (39–52)	54 (35;72)	65 (49;82)	64 (56;72)	62 (53;70)	66 (63;70)
#4	45 (30–60)	45 (26–60)	39 (22–60)	56 (40–74)	92 (88;96)	89 (75;103)	81 (65;96)	66 (53;78)	67 (52; 83)
#5	33 (21–52)	37 (25–50)	39 (23–56)	44 (37–57)	61 (60;63)	78 (70;86)	73 (65;80)	49 (37;60)	55 (42;68)
#6	47 (21–82)	50 (36–63)	43 (15–61)	53 (34–68)	79 (74;84)	75 (68;83)	91 (87;96)	71 (65;76)	67 (61;74)
#7	46 (24–85)	57 (32–85)	43 (33–64)	38 (32–42)	55 (46;64)	61 (52;70)	58 (52;65)	42 (37;47)	55 (52;58)
#8	55 (33–79)	58 (40–80)	68 (24–116)	74 (50–92)	80 (68;93)	92 (88;95)	112 (100;124 *)	107 (95;119)	79 (50;109)
#9	40 (21–61)	45 (29–59)	58 (30–84)	64 (38–82)	67 (64;70)	78 (75;82)	92 (82;102)	92 (75;110)	84 (70;98)
#10	36 (17–66)	44 (19–64)	46 (33–55)	40 (30–57)	46 (45;47)	59 (49;68)	59 (53;65)	58 (49;68)	63 (63;63)

M marginal; AMA axio-marginal-angle; A axial; AOA axio-occlusal-angle; O1 occlusal 1; O2 occlusal 2; O3 occlusal 3; O4 occlusal 4; O5 occlusal 5; * indicates an individually measured value equal to or exciding 120 μm at the certain measurement point.

The UI analysis revealed that group ZI had a significantly more uniform (closer to ideal) internal fit than group ZE (The closer the ratio to 1, the more uniform the internal cement space) (Figure 7).
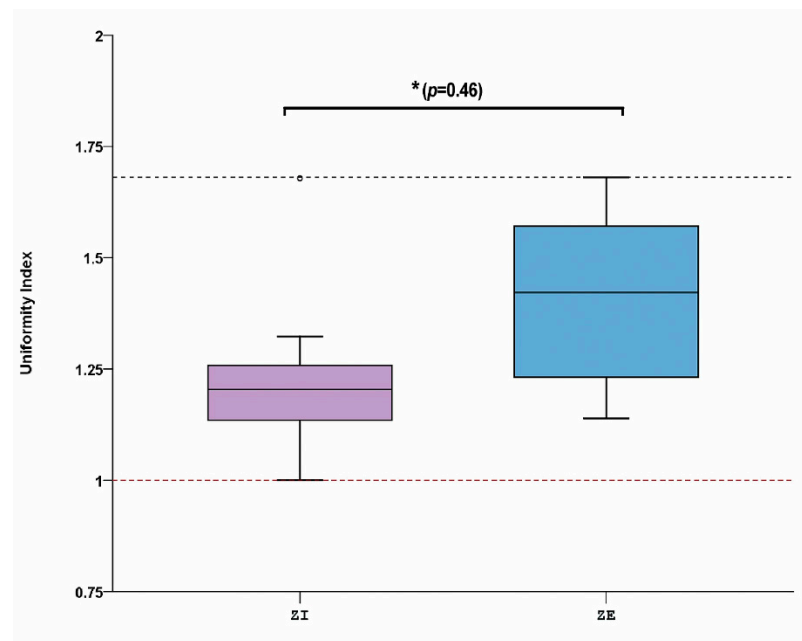
Figure 7. Uniformity index results for compared groups (ZI and ZE) (closer results to 1 mean more uniform internal spacing). * indicates significance (*p* < 0.05 according to Independent Samples *t*-test).

4. Discussion

The results of the present study revealed that marginal and internal gap values of CAD-CAM monolithic zirconia crowns fabricated by using a completely digital production workflow were significantly smaller than those of a semi-digital workflow. Thus, the null hypothesis was rejected.

The results obtained through the completely digital workflow used in this study could not be directly compared with the previous study results because IOSs, software, and evaluation methods utilized varied across studies [41,42]. Additionally, to the authors' knowledge, studies with similar materials and methodology were either scarce or lacking. Nevertheless, the results derived from this study are in accordance with some previous studies [41,42,51,52]. Group ZI had significantly better marginal and internal fit at all measurement locations than group ZE. Haddadi et al. [51] also reported marginal and internal fit in favor of a completely digital workflow in a split-mouth randomized clinical study for lithium disilicate crowns. Uluc et al. [52] reported similar but not statistically significant in vitro results for 5-unit zirconia FDPs. Sakornwimon et al. [41] and Freire et al. [42] evaluated IOS vs. EOS concerning only the marginal fit of monolithic zirconia crowns and found no significant difference. However, IOS enabled lower marginal gap values.

Overall mean gap values calculated in this study ranged between 29 and 43 μm for completely digital workflow and 42 and 75 μm for semi-digital workflow. Freire et al. [42] presented similar mean marginal gap values for both workflows, whereas other above-mentioned studies [41,51,52] reported mean marginal gap values of 62–72 μm for IOS and 57–83 μm for EOS and mean axial and occlusal gap values of 75–162 μm for IOS and 82–182 for EOS. Present study results are relatively lower than those, hence are promising.

Recent studies [46,47,53–55] which investigated the marginal and/or internal fit of monolithic zirconia crowns fabricated only by semi-digital workflow reported results which were not better than those in the present study. Paul et al. [55] presented mean marginal gap values of 77 μm and mean axial and occlusal gap values of 57–105 μm. Schriwer et al. [53] reported mean axial and occlusal gap values of 50–142 μm. The results of Rau et al. [44] for marginal and internal fit ranged between 101 and 104 μm. The results of Sadeqi et al. [46] were 38 μm for the marginal gap and 142 μm for the mean overall internal fit. Ha and Cho [47] reported a marginal gap range of 64–66 μm, which was 44–70 μm for axial, and 171–213 μm for occlusal gaps.

The current study presented gradually increasing gap values from the margins through axial walls up to the occlusal surface. Many studies [47,49,51–53,55] have reported similar variations focusing mainly on the difference between the axial and occlusal gap. This phenomenon has been attributed to the insufficient compensation of digitally calculated shrinkage incorporated in 3D virtual models by the actual shrinkage occurring during the sintering process after milling [53].

The gap value of 120 μm was considered as a reference for clinical acceptability in the present study, and misfits equal to or exceeding 120 μm at each measurement point per specimen were reported to avoid misleading conclusions [56]. The mean values calculated at any measurement location for both tested groups (ZI and ZE) in this study were all within the clinically acceptable limit of 120 μm. Moreover, individually measured gap values exceeding 100 μm were at 7 points, and only 1 of these values (124 μm) was over 120 μm. All of these peak values measured in group ZE were mainly at the occlusal part, clustering on three specimens, and four values were detected in one specimen alone. As only one specimen had most of the higher values, this specimen may be responsible for the higher mean values in the ZE group.

The UI analysis performed in the present study had close to ideal index results for both groups, with the statistical difference in favor of group ZI. In addition to overall clinically acceptable gap values calculated for groups ZI and ZE, the UI results have gained significance.

Compared workflows performed well within the clinically acceptable range, and yet, completely digital workflow incorporating IOS presented significantly better results. Previous studies claim digital workflow to be overall more comfortable and tolerable for the patient, thereby being the preferred way for fixed prosthodontic treatment [41,57,58].

The current study used the 2D silicon replica technique to evaluate the marginal and internal fit of the crowns. Being a well-established methodology in the literature [32,41,42,44,47,49,51–55], it has been defined as an easy, reproducible, and economical method applicable to both in vitro and in vivo studies [42,47,49,52]. The main limitation of the technique is the reduced number of available areas for analysis and being operator-dependent, which may result in difficulties in their standardization and results not representing an ideal overall evaluation [42,49]. However, it is a non-invasive, physical technique to mimic the cement thickness as a result of the cementation process that takes place in the clinic [48,59]. Digital analysis of fit has been recently available; however, this technique requires appropriate software, which may be costly and also depend on the accuracy of the scan and superimposition algorithm [60,61].

In an attempt to reproduce clinical conditions, finger pressure was used in the current study to seat the crowns. This technique and the application of as low as 8–10 N load static pressure has been adapted by some previous studies [32,42,47,52]. It has been reported that higher seating forces have no effect on the cement thickness statistically [62].

The current study adopted the marginal gap as the evaluation parameter for the marginal fit of the restorations because a substantial misfit at the vertical marginal component of the absolute marginal gap would result in harder to adjust inadaptability that most often would require the remaking of the restoration [25,56]. Whereas horizontal over-extensions might be improved by recontouring the margins [56], and under-extensions might be improved by adding some veneering ceramic to the zirconia material.

Uniformity of internal cement space has become a point of interest in recent years [49,50]. UI analysis was performed in the present study to evaluate the uniformity of the internal fit and to complement the marginal and internal fit results. Currently, data regarding UI evaluation methodology is limited [50].

Above-discussed studies used varying ceramic brands and systems, sintering processes, simulated cement space settings of 40–50 μm, different mediums for the fixation of the restorations via low-viscosity silicon (silicon replica technique) or cement, different CAD-CAM systems, IOSs, EOSs, and software. Therefore, the results of the present study should be interpreted with caution, considering that one type of zirconia brand, CAD-CAM

system, IOS, EOS, and their corresponding software, were used with a relatively small sample size. The results of the present study should be corroborated with clinical data.

5. Conclusions

Within the limitations of this in vitro study, the following conclusions were drawn:

1. Completely digital workflow resulted in smaller marginal and internal gaps along with improved internal fit uniformity compared with the tested combination of conventional and digital workflows (semi-digital).

2. Completely digital and semi-digital workflows provided acceptable marginal and internal fit for CAD-CAM monolithic zirconia molar crowns (<120 μm).

References

1. Blatz, M.B.; Conejo, J. The current state of chairside digital dentistry and materials. *Dent. Clin. N. Am.* **2019**, *63*, 175–197. [CrossRef] [PubMed]
2. Abduo, J.; Elseyoufi, M. Accuracy of intraoral scanners: A systematic review of influencing factors. *Eur. J. Prosthodont. Restor. Dent.* **2018**, *26*, 101–121. [CrossRef] [PubMed]
3. Mangano, F.; Gandolfi, A.; Luongo, G.; Logozzo, S. Intraoral scanners in dentistry: A review of the current literature. *BMC Oral Health* **2017**, *17*, 149. [CrossRef] [PubMed]
4. Siqueira, R.; Galli, M.; Chen, Z.; Mendonça, G.; Meirelles, L.; Wang, H.L.; Chan, H.L. Intraoral scanning reduces procedure time and improves patient comfort in fixed prosthodontics and implant dentistry: A systematic review. *Clin. Oral Investig.* **2021**, *25*, 6517–6531. [CrossRef] [PubMed]
5. Ammoun, R.; Suprono, M.S.; Goodacre, C.J.; Oyoyo, U.; Carrico, C.K.; Kattadiyil, M.T. Influence of tooth preparation design and scan angulations on the accuracy of two intraoral digital scanners: An in vitro study based on 3-dimensional comparisons. *J. Prosthodont.* **2020**, *29*, 201–206. [CrossRef] [PubMed]
6. Leitão, C.I.M.B.; Fernandes, G.V.O.; Azevedo, L.P.P.; Araújo, F.M.; Donato, H.; Correia, A.R.M. Clinical performance of monolithic CAD/CAM tooth-supported zirconia restorations: Systematic review and meta-analysis. *J. Prosthodont. Res.* **2022**, *66*, 374–384. [CrossRef]
7. de Kok, P.; Kleverlaan, C.J.; de Jager, N.; Kuijs, R.; Feilzer, A.J. Mechanical performance of implant-supported posterior crowns. *J. Prosthet. Dent.* **2015**, *114*, 59–66. [CrossRef]
8. Nakamura, K.; Harada, A.; Inagaki, R.; Kanno, T.; Niwano, Y.; Milleding, P.; Örtengren, U. Fracture resistance of monolithic zirconia molar crowns with reduced thickness. *Acta. Odontol. Scand.* **2015**, *73*, 602–608. [CrossRef]
9. Ramos, G.F.; Monteiro, E.B.; Bottino, M.A.; Zhang, Y.; Marques de Melo, R. Failure probability of three designs of zirconia crowns. *Int. J. Periodontics Restor. Dent.* **2015**, *35*, 843–849. [CrossRef]
10. Sorrentino, R.; Triulzio, C.; Tricarico, M.G.; Bonadeo, G.; Gherlone, E.F.; Ferrari, M. In vitro analysis of the fracture resistance of CAD-CAM monolithic zirconia molar crowns with different occlusal thickness. *J. Mech. Behav. Biomed. Mater.* **2016**, *61*, 328–333. [CrossRef]
11. Sulaiman, T.A.; Abdulmajeed, A.A.; Donovan, T.E.; Cooper, L.F.; Walter, R. Fracture rate of monolithic zirconia restorations up to 5 years: A dental laboratory survey. *J. Prosthet. Dent.* **2016**, *116*, 436–439. [CrossRef] [PubMed]
12. Cionca, N.; Hashim, D.; Mombelli, A. Zirconia dental implants: Where are we now, and where are we heading? *Periodontol. 2000* **2017**, *73*, 241–258. [CrossRef] [PubMed]
13. Griffin, J.D., Jr. Combining monolithic zirconia crowns, digital impressioning, and regenerative cement for a predictable restorative alternative to PFM. *Compend. Contin. Educ. Dent.* **2013**, *34*, 212–222. [PubMed]

14. Mazza, L.C.; Lemos, C.A.A.; Pesqueira, A.A.; Pellizzer, E.P. Survival and complications of monolithic ceramic for tooth-supported fixed dental prostheses: A systematic review and meta-analysis. *J. Prosthet. Dent.* **2021**, *128*, 566–574. [CrossRef]

15. Laumbacher, H.; Strasser, T.; Knüttel, H.; Rosentritt, M. Long-term clinical performance and complications of zirconia-based tooth- and implant-supported fixed prosthodontic restorations: A summary of systematic reviews. *J. Dent.* **2021**, *111*, 103723. [CrossRef]

16. Abduo, J.; Lyons, K.; Swain, M. Fit of zirconia fixed partial denture: A systematic review. *J. Oral Rehabil.* **2010**, *37*, 866–876. [CrossRef]

17. Hunter, A.J.; Hunter, A.R. Gingival margins for crowns: A review and discussion. Part II: Discrepancies and configurations. *J. Prosthet. Dent.* **1990**, *64*, 636–642. [CrossRef]

18. Karlsson, S. The fit of Procera titanium crowns. An in vitro and clinical study. *Acta. Odontol. Scand.* **1993**, *51*, 129–134. [CrossRef]

19. Contrepois, M.; Soenen, A.; Bartala, M.; Laviole, O. Marginal adaptation of ceramic crowns: A systematic review. *J. Prosthet. Dent.* **2013**, *110*, 447–454. [CrossRef]

20. Boitelle, P.; Mawussi, B.; Tapie, L.; Fromentin, O. A systematic review of CAD/CAM fit restoration evaluations. *J. Oral Rehabil.* **2014**, *41*, 853–874. [CrossRef]

21. Tuntiprawon, M.; Wilson, P.R. The effect of cement thickness on the fracture strength of all-ceramic crowns. *Aust. Dent. J.* **1995**, *40*, 17–21. [CrossRef] [PubMed]

22. Wiskott, H.W.; Belser, U.C.; Scherrer, S.S. The effect of film thickness and surface texture on the resistance of cemented extracoronal restorations to lateral fatigue loading. *Int. J. Prosthodont.* **1999**, *12*, 255–262. [PubMed]

23. May, L.G.; Kelly, J.R.; Bottino, M.A.; Hill, T. Effects of cement thickness and bonding on the failure loads of CAD/CAM ceramic crowns: Multi-physics FEA modeling and monotonic testing. *Dent. Mater.* **2012**, *28*, E99–E109. [CrossRef] [PubMed]

24. Borba, M.; Cesar, P.F.; Griggs, J.A.; Della Bona, A. Adaptation of all-ceramic fixed partial dentures. *Dent. Mater.* **2011**, *27*, 1119–1126. [CrossRef] [PubMed]

25. Holmes, J.R.; Bayne, S.C.; Holland, G.A.; Sulik, W.D. Considerations in measurement of marginal fit. *J. Prosthet. Dent.* **1989**, *62*, 405–408. [CrossRef]

26. Holmes, J.R.; Sulik, W.D.; Holland, G.A.; Bayne, S.C. Marginal fit of castable ceramic crowns. *J. Prosthet. Dent.* **1992**, *67*, 594–599. [CrossRef]

27. McLean, J.W.; von Frauenhofer, J.A. The estimation of cement film thickness by an in vivo technique. *Br. Dent. J.* **1971**, *131*, 107–111. [CrossRef]

28. Sorensen, J.A. A standardized method for determination of crown margin fidelity. *J. Prosthet. Dent.* **1990**, *64*, 18–24. [CrossRef]

29. Karataşli, O.; Kursoğlu, P.; Capa, N.; Kazazoğlu, E. Comparison of the marginal fit of different coping materials and designs produced by computer aided manufacturing systems. *Dent. Mater. J.* **2011**, *30*, 97–102. [CrossRef]

30. Matta, R.E.; Schmitt, J.; Wichmann, M.; Holst, S. Circumferential fit assessment of CAD/CAM single crowns—A pilot investigation on a new virtual analytical protocol. *Quintessence Int.* **2012**, *43*, 801–809.

31. Euán, R.; Figueras-Álvarez, O.; Cabratosa-Termes, J.; Oliver-Parra, R. Marginal adaptation of zirconium dioxide copings: Influence of the CAD/CAM system and the finish line design. *J. Prosthet. Dent.* **2014**, *112*, 155–162. [CrossRef] [PubMed]

32. Souza, R.O.A.; Özcan, M.; Pavanelli, C.A.; Buso, L.; Lombardo, G.H.L.; Michida, S.M.A.; Mesquita, A.M. Marginal and internal discrepancies related to margin design of ceramic crowns fabricated by a CAD/CAM system. *J. Prosthodont.* **2012**, *21*, 94–100. [CrossRef] [PubMed]

33. Kocaagaoglu, H.; Kilinc, H.I.; Albayrak, H. Effect of digital impressions and production protocols on the adaptation of zirconia copings. *J. Prosthet. Dent.* **2017**, *117*, 102–108. [CrossRef] [PubMed]

34. Dauti, R.; Cvikl, B.; Franz, A.; Schwarze, U.Y.; Lilaj, B.; Rybaczek, T.; Moritz, A. Comparison of marginal fit of cemented zirconia copings manufactured after digital impression with Lava™ C.O.S and conventional impression technique. *BMC Oral Health* **2016**, *16*, 129. [CrossRef] [PubMed]

35. Pedroche, L.O.; Bernardes, S.R.; Leão, M.P.; de Almeida Kintopp, C.C.; Correr, G.M.; Ornaghi, B.P.; Gonzaga, C.C. Marginal and internal fit of zirconia copings obtained using different digital scanning methods. *Braz. Oral Res.* **2016**, *30*, e113. [CrossRef]

36. Rödiger, M.; Heinitz, A.; Bürgers, R.; Rinke, S. Fitting accuracy of zirconia single crowns produced via digital and conventional impressions-a clinical comparative study. *Clin. Oral Investig.* **2017**, *21*, 579–587. [CrossRef]

37. Kohorst, P.; Brinkmann, H.; Dittmer, M.P.; Borchers, L.; Stiesch, M. Influence of the veneering process on the marginal fit of zirconia fixed dental prostheses. *J. Oral Rehabil.* **2010**, *37*, 283–291. [CrossRef]

38. Pak, H.S.; Han, J.S.; Lee, J.B.; Kim, S.H.; Yang, J.H. Influence of porcelain veneering on the marginal fit of Digident and Lava CAD/CAM zirconia ceramic crowns. *J. Adv. Prosthodont.* **2010**, *2*, 33–38. [CrossRef]

39. Torabi, K.; Vojdani, M.; Giti, R.; Taghva, M.; Pardis, S. The effect of various veneering techniques on the marginal fit of zirconia copings. *J. Adv. Prosthodont.* **2015**, *7*, 233–239. [CrossRef]

40. Ahmed, W.M.; Abdallah, M.N.; McCullagh, A.P.; Wyatt, C.C.L.; Troczynski, T.; Carvalho, R.M. Marginal discrepancies of monolithic zirconia crowns: The influence of preparation designs and sintering techniques. *J. Prosthodont.* **2019**, *28*, 288–298. [CrossRef]

41. Sakornwimon, N.; Leevailoj, C. Clinical marginal fit of zirconia crowns and patients' preferences for impression techniques using intraoral digital scanner versus polyvinyl siloxane material. *J. Prosthet. Dent.* **2017**, *118*, 386–391. [CrossRef] [PubMed]

42. Freire, Y.; Gonzalo, E.; Lopez-Suarez, C.; Pelaez, J.; Suarez, M.J. Evaluation of the marginal fit of monolithic crowns fabricated by direct and indirect digitization. *J. Prosthodont. Res.* **2021**, *65*, 291–297. [CrossRef] [PubMed]

43. Rosenstiel, S.F.; Land, M.F.; Fujimoto, J. *Contemporary Fixed Prosthodontics*, 5th ed.; Elsevier: St. Louis, MO, USA, 2016; pp. 264–277.

44. Tamac, E.; Toksavul, S.; Toman, M. Clinical marginal and internal adaptation of CAD/CAM milling, laser sintering, and cast metal ceramic crowns. *J. Prosthet. Dent.* **2014**, *112*, 909–913. [CrossRef] [PubMed]

45. Kale, E.; Yilmaz, B.; Seker, E.; Özcelik, T.B. Effect of fabrication stages and cementation on the marginal fit of CAD-CAM monolithic zirconia crowns. *J. Prosthet. Dent.* **2017**, *118*, 736–741. [CrossRef] [PubMed]

46. Sadeqi, H.A.; Baig, M.R.; Al-Shammari, M. Evaluation of marginal/internal fit and fracture load of monolithic zirconia and zirconia lithium silicate (ZLS) CAD/CAM crown systems. *Materials* **2021**, *14*, 6346. [CrossRef]

47. Ha, S.J.; Cho, J.H. Comparison of the fit accuracy of zirconia-based prostheses generated by two CAD/CAM systems. *J. Adv. Prosthodont.* **2016**, *8*, 439–448. [CrossRef] [PubMed]

48. Davis, S.H.; Kelly, J.R.; Campbell, S.D. Use of an elastomeric material to improve the occlusal seat and marginal seal of cast restorations. *J. Prosthet. Dent.* **1989**, *62*, 288–291. [CrossRef]

49. Ferrairo, B.M.; Piras, F.F.; Lima, F.F.; Honório, H.M.; Duarte, M.A.H.; Borges, A.F.S.; Rubo, J.H. Comparison of marginal adaptation and internal fit of monolithic lithium disilicate crowns produced by 4 different CAD/CAM systems. *Clin. Oral Investig.* **2021**, *25*, 2029–2036. [CrossRef]

50. Li, Y.; Zhao, J.; Sun, Z.; Lin, N.; Zheng, Y. Three-dimensional fit of self-glazed zirconia monolithic crowns fabricated by wet deposition. *Dent. Mater. J.* **2022**, *41*, 363–367. [CrossRef]

51. Haddadi, Y.; Bahrami, G.; Isidor, F. Accuracy of crowns based on digital intraoral scanning compared to conventional impression-a split-mouth randomised clinical study. *Clin. Oral Investig.* **2019**, *23*, 4043–4050. [CrossRef]

52. Uluc, I.G.; Guncu, M.B.; Aktas, G.; Turkyilmaz, I. Comparison of marginal and internal fit of 5-unit zirconia fixed dental prostheses fabricated with CAD/CAM technology using direct and indirect digital scans. *J. Dent. Sci.* **2022**, *17*, 63–69. [CrossRef] [PubMed]

53. Schriwer, C.; Skjold, A.; Gjerdet, N.R.; Øilo, M. Monolithic zirconia dental crowns. Internal fit, margin quality, fracture mode and load at fracture. *Dent. Mater.* **2017**, *33*, 1012–1020. [CrossRef]

54. Rau, S.A.; Raedel, M.; Mikeli, A.; Raedel, M.; Walter, M.H. Clinical fit of monolithic zirconia single crowns. *Int. J. Prosthodont.* **2018**, *31*, 443–445. [CrossRef] [PubMed]

55. Paul, N.; Raghavendra Swamy, K.N.; Dhakshaini, M.R.; Sowmya, S.; Ravi, M.B. Marginal and internal fit evaluation of conventional metal-ceramic versus zirconia CAD/CAM crowns. *J. Clin. Exp. Dent.* **2020**, *12*, e31–e37. [CrossRef] [PubMed]

56. Kale, E.; Seker, E.; Yilmaz, B.; Ozcelik, T.B. Effect of cement space on the marginal fit of CAD/CAM-fabricated monolithic zirconia crowns. *J. Prosthet. Dent.* **2016**, *116*, 890–895. [CrossRef] [PubMed]

57. Yuzbasioglu, E.; Kurt, H.; Turunc, R.; Bilir, H. Comparison of digital and conventional impression techniques: Evaluation of patients' perception, treatment comfort, effectiveness and clinical outcomes. *BMC Oral Health* **2014**, *14*, 10. [CrossRef]

58. Schepke, U.; Meijer, H.J.; Kerdijk, W.; Cune, M.S. Digital versus analog complete-arch impressions for single-unit premolar implant crowns: Operating time and patient preference. *J. Prosthet. Dent.* **2015**, *114*, 403–406.e1. [CrossRef]

59. Berrendero, S.; Salido, M.P.; Valverde, A.; Ferreiroa, A.; Pradíes, G. Influence of conventional and digital intraoral impressions on the fit of CAD/CAM-fabricated all-ceramic crowns. *Clin. Oral Investig.* **2016**, *20*, 2403–2410. [CrossRef]

60. Anadioti, E.; Aquilino, S.A.; Gratton, D.G.; Holloway, J.A.; Denry, I.; Thomas, G.W.; Qian, F. 3D and 2D marginal fit of pressed and CAD/CAM lithium disilicate crowns made from digital and conventional impressions. *J. Prosthodont.* **2014**, *23*, 610–617. [CrossRef]

61. Zimmermann, M.; Valcanaia, A.; Neiva, G.; Mehl, A.; Fasbinder, D. Digital evaluation of the fit of zirconia-reinforced lithium silicate crowns with a new three-dimensional approach. *Quintessence Int.* **2018**, *49*, 9–15. [CrossRef]

62. Weaver, J.D.; Johnson, G.H.; Bales, D.J. Marginal adaptation of castable ceramic crowns. *J. Prosthet. Dent.* **1991**, *66*, 747–753. [CrossRef] [PubMed]